

# Dynamics and pattern formation in invasive tumor growth

Evgeniy Khain and Leonard M. Sander

Department of Physics and Michigan Center for Theoretical Physics,  
The University of Michigan, Ann Arbor, Michigan 48109

In this work, we study the *in-vitro* dynamics of the most malignant form of the primary brain tumor: Glioblastoma Multiforme. Typically, the growing tumor consists of the inner dense proliferating zone and the outer less dense invasive region. Experiments with different types of cells show qualitatively different behavior. Wild-type cells invade a spherically symmetric manner, but mutant cells are organized in tenuous branches. We formulate a model for this sort of growth using two coupled reaction-diffusion equations for the cell and nutrient concentrations. When the ratio of the nutrient and cell diffusion coefficients exceeds some critical value, the plane propagating front becomes unstable with respect to transversal perturbations. The instability threshold and the full phase-plane diagram in the parameter space are determined. The results are in a good agreement with experimental findings for the two types of cells.

PACS numbers: 87.18.Ed, 87.18.Hf

One of the most aggressive forms of primary brain tumor is Glioblastoma Multiforme (GBM) [1]. Despite major advances in medical science the prognosis for victims of this disease is very poor [1]: the median survival for patients with newly diagnosed GBM is approximately 12 months. One of the main reasons for such high mortality and poor success of treatment is the fact that GBMs are highly invasive [2]. The growing tumor sheds invasive cells which run through the brain, see Fig. 1. The invasive nature of malignant gliomas makes treatment difficult [2]; secondary tumors are produced by the invasive cells even if the primary is removed. In this paper we introduce a reaction-diffusion model for invasion. By comparing two different cell lines we hope to get insight into invasion dynamics which is needs to be better understood.

This work is inspired by recent *in vitro* experiments [5, 6] where microscopic tumor spheroids (radius about  $250\ \mu$ ) were placed in collagen-I gel and allowed to grow. The cell lines used were U87 and U87- $\Delta$ EGFR. The first type is called ‘wild-type’ in what follows. The second is a mutant line [4] in which there is an amplification of the epidermal growth factor receptor (EGFR) gene. This amplification occurs in approximately 40 percent of cases of GBM [3].

If we compare the growth of the two cell lines *in vitro* we see two main differences; cf. Figure 1. The invasive region for the wild-type cells grows faster than for the mutant cells, and the wild-type produces a spherically symmetric pattern, whereas mutant cells produce a branching pattern [6]. In the present work, we formulate a simple reaction-diffusion model that is able to reproduce these experimental findings and may give insight into the functional significance of the mutation.

We interpret the branching shown in Fig. 1b, as a branching instability. Analogous instabilities were studied in the theory of combustion [7], and in studies of the self-organization of microorganisms [8]. One way of modeling this is to assume that there is attraction between

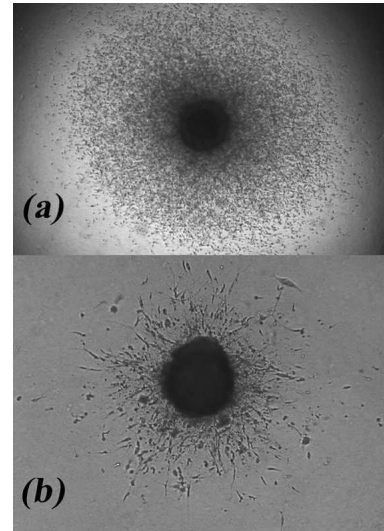


FIG. 1: Growing tumors from *in vitro* experiments [6] in collagen gel for the wild-type (a) and mutant (b) cells. These *in vitro* tumors consist of an inner proliferation zone with a very high density of cells and an outer invasive zone, where the cell density is smaller. The structure *in vivo* is believed to be similar. The radius of the inner zone here is about  $250\ \mu$ . For wild-type cells a spherically symmetric pattern is observed, (a). Mutant cells are organized in tenuous branches, (b). Note also that the invasive region for the mutant type cells grows slower than for wild-type cells.

cells [9] due to the production of growth factors. Another possibility is to assume nonlinear diffusion, where the diffusion coefficient *increases* with the density of the cells, as was proposed for bacterial colonies [8]. We will introduce another mechanism based on the known biology of GBM.

In our continuum description, we will deal with the density of cells  $u(\mathbf{r}, t)$  and the density of some growth factor or nutrient (whichever controls the growth),  $c(\mathbf{r}, t)$ . We assume that  $c$  diffuses to the tumor from far away. Each cancer cell is able to proliferate as well as to per-

form random motion. It is known that within the inner region, cells have quite a high proliferation rate whereas in the invasive region, cells have high motility, but low proliferation rate [10]. This is an indication of a dynamical switch between the cell phenotypes [10]. We model it by introducing a *density-dependent* proliferation term where the proliferation rate increases with cell density. The simplest form for such a term is  $\partial u / \partial t \propto u^2 c$ . (The extra power of  $u$  compared to the usual  $uc$  means that high density gives rapid proliferation since the proliferation rate per cell,  $(1/u)\partial u / \partial t \propto u$ .) As we will see, this term drives the instability and leads to branching. We assume that in order to proliferate a cell needs to consume some amount of  $c$ . The density  $c$  obeys a diffusion equation with a sink at the tumor cells.

We encode these assumptions in the following equations:

$$\begin{aligned} \frac{\partial u}{\partial t} &= \nabla \cdot (D_u \nabla u) + \alpha u^2 c, \\ \frac{\partial c}{\partial t} &= \nabla \cdot (D_c \nabla c) - \beta u^2 c. \end{aligned} \quad (1)$$

Here  $D_u$  and  $D_c$  are the diffusion coefficients of  $u$  and  $c$ ,  $\alpha$  is a proliferation coefficient, and  $\beta$  is the coefficient of nutrient consumption. We assume that the density in the center of the tumor is not very high compared to the density of closely packed cells  $u_c$ . We suppose also that the nutrient concentration is kept constant far from the tumor:  $\lim_{r \rightarrow \infty} c(r) = c_\infty$ .

In what follows we will measure cell density in the units of some characteristic density  $u_0$ , nutrient density in units of  $c_\infty$ , distance in units of  $[D_c / (\beta u_0^2)]^{1/2}$ , and time in units of  $(\beta u_0^2)^{-1}$ . This gives:

$$\begin{aligned} \frac{\partial u}{\partial t} &= \frac{1}{\delta} \nabla^2 u + \frac{1}{m} u^2 c, \\ \frac{\partial c}{\partial t} &= \nabla^2 c - u^2 c, \end{aligned} \quad (2)$$

where  $\delta = D_c / D_u$  is the ratio of the nutrient and cell diffusion coefficients and  $m = \beta u_0 / (\alpha c_\infty)$  is the ratio of consumption and proliferation rates.

Typically, the nutrient or growth factor represented by  $c$  is a small molecule. It is expected to diffuse much faster than the cells. For example, the diffusion coefficient of glucose in the brain is of the order of  $10^{-7} \text{cm}^2/\text{s}$ , while the cell diffusion is of the order of  $10^{-9} \text{cm}^2/\text{s}$  [9], so that  $\delta \sim 100$ . A typical nutrient consumption is  $10^{-12} \text{g/cell/min}$  [11], and a typical glucose concentration is of the order of  $1 \text{g/l}$ . Assuming that typical cell density within the invasive region is of the order of  $10^5 \text{cell/cm}^3$ , we estimate the consumption rate as  $1.7 \times 10^{-6} \text{s}^{-1}$ . The typical proliferation rate in experiments [6] is of the order of  $1/\text{day}$ , so that  $m$  turns out to be of the order of  $0.1$ .

We work in a two-dimensional channel geometry. Let  $x$  be the direction of tumor growth, and  $y$  be the transverse direction, perpendicular to the direction of the front

propagation. In the  $y$  direction we use periodic boundary conditions with a finite channel width. In the  $x$  direction, far ahead of the tumor, the cell concentration is zero,  $u(x = \infty) = 0$ , and the scaled nutrient concentration is unity,  $c(x = \infty) = 1$ . On the other hand, at  $x = -\infty$  we demand  $c = 0$ . There is a conservation law in Eqs. (2): a volume integral over the system of  $(mu + c)$  is a conserved quantity. Its interpretation is that in our model a cell needs some amount of food to divide. Therefore, at  $x = -\infty$ ,  $u = 1/m$  if there is a steady state. Our initial conditions are  $u = 1/m$  for  $x \leq 0$ ;  $u = 0$  for  $x > 0$ , and  $c = 0$ , for  $x \leq 0$ ;  $c = c_\infty$  for  $x > 0$ . We will investigate the situation after transients have died away and a steady propagating state has been established.

First, we consider the solutions of Eqs. (2) in the form of plane propagating fronts:  $u = u_0(\xi)$ ;  $c = c_0(\xi)$ ,  $\xi = x - vt$ . Substituting into Eqs. (2) we arrive at:

$$\begin{aligned} \frac{1}{\delta} u_0'' + v u_0' + \frac{1}{m} u_0^2 c_0 &= 0, \\ c_0'' + v c_0' - u_0^2 c_0 &= 0. \end{aligned} \quad (3)$$

To obtain the profiles and the velocity of front propagation, we performed (in Matlab) the following shooting procedure. First, we write down Eqs. (3) as four coupled first-order differential equations in the form  $(\vec{a})' = M(\vec{a})$ , where  $\vec{a}$  is the column of solutions with elements  $u_0, u_0', c_0, c_0'$ . Then we find the eigenvalues and eigenvectors of  $M$  at  $\xi = \pm\infty$ . Starting with the solution  $\vec{a}$  that is proportional to the eigenvector belonging to the positive eigenvalue at  $\xi = -\infty$  (using the linearity of the problem, we choose the constant of proportionality to be unity), we perform shooting by the velocity of front propagation  $v$ . We find the profiles by demanding that the solution  $\vec{a}$  at  $\xi = +\infty$  is a linear combination of the two eigenvectors  $\vec{\psi}_1$  and  $\vec{\psi}_2$  belonging to negative eigenvalues  $\lambda_1$  and  $\lambda_2$  at  $\xi = +\infty$ :  $\vec{a} = b_1 \vec{\psi}_1 \exp(\lambda_1 \xi) + b_2 \vec{\psi}_2 \exp(\lambda_2 \xi)$ . Figure 2 shows a typical solution of Eqs. (3) for  $u = u(\xi)$  and  $c = c(\xi)$ .

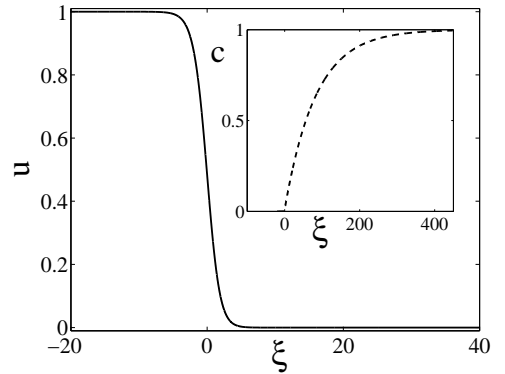


FIG. 2: Density profiles of cells and nutrient from Eqs. (3). The first curve is the cell density  $u = u(\xi)$  (solid line.) The second curve (dashed) is  $c = c(\xi)$  (inset). The parameters are  $m = 1$ ,  $\delta = 100$ .

We now perform a linear stability analysis. Consider perturbations in the transverse direction

$$\begin{aligned} u &= u_0(\xi) + u_1(\xi) \exp(\gamma t + iky), \\ c &= c_0(\xi) + c_1(\xi) \exp(\gamma t + iky) \end{aligned} \quad (4)$$

and substitute into Eqs. (2). We have

$$\begin{aligned} \frac{1}{\delta} u_1'' + v u_1' + \left( \frac{2}{m} c_0 u_0 - \frac{k^2}{\delta} - \gamma \right) u_1 + \frac{1}{m} u_0^2 c_1 &= 0, \\ c_1'' + v c_1' - (u_0^2 + k^2 + \gamma) c_1 - 2c_0 u_0 u_1 &= 0. \end{aligned} \quad (5)$$

For a fixed value of transverse wave number  $k$ , we should find the perturbations  $u_1(\xi)$  and  $c_1(\xi)$ , and the growth rate  $\gamma$ . As before, we rewrite Eqs. (5) as four coupled first-order differential equations in the form  $(\vec{a}_{lin})' = M_{lin}(\vec{a}_{lin})$ . There are two positive eigenvalues of the matrix  $M_{lin}$  at  $\xi = -\infty$ . We start at  $\xi = -\infty$  from the linear combination of the corresponding eigenvectors,  $\vec{a}_{lin} = b_3 \vec{\psi}_3 \exp(\lambda_3 \xi) + b_4 \vec{\psi}_4 \exp(\lambda_4 \xi)$ , where one can choose  $b_4$  to be unity due to the linearity of the problem. Performing shooting in two parameters, the growth rate  $\gamma$  and the constant  $b_3$ , we find the eigenfunctions  $u_1(\xi)$  and  $c_1(\xi)$  by demanding that the solution  $\vec{a}_{lin}$  is given at  $\xi = +\infty$  by a linear combination of the two eigenvectors  $\vec{\psi}_5$  and  $\vec{\psi}_6$  belonging to negative eigenvalues  $\lambda_5$  and  $\lambda_6$ ,  $\vec{a}_{lin} = b_5 \vec{\psi}_5 \exp(\lambda_5 \xi) + b_6 \vec{\psi}_6 \exp(\lambda_6 \xi)$ . Changing the value of transverse wave number  $k$ , for the fixed  $\delta$  and  $m$ , we calculate the dispersion curve  $\gamma(k)$ .

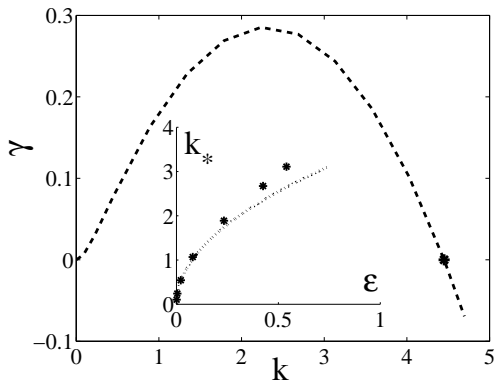


FIG. 3: An example of the dispersion curve  $\gamma(k)$ . The instability occurs if the ratio of diffusion coefficients  $\delta$  exceeds a certain critical value. For  $\delta > \delta_{cr} \approx 2.300$ , the growth rate  $\gamma$  is positive for small  $k$ , while for larger  $k$ , cell diffusion in the transverse direction stabilizes the instability. The parameters are:  $m = 0.1$ ,  $\delta = 20$ . The inset shows the dependence of the largest unstable wave number  $k_*$  on  $\epsilon = (\delta - \delta_{cr})/\delta_{cr}$ . Numerical simulations are the asterisks, the asymptote  $k_* = (0.36/m)\epsilon^{1/2}$  is the dotted line.

As was found previously in the context of chemical reactions for  $m = 1$  [12], plane fronts can become transversally unstable if the ratio of diffusion coefficients  $\delta$  exceeds a certain critical value. Indeed, for  $\delta > \delta_{cr}$ , the growth rate  $\gamma$  is positive for small  $k$ , while for larger

$k$ , cell diffusion in the transverse direction stabilizes the instability. We checked that  $\delta_{cr} \approx 2.300$ , in agreement with previous results [12, 13]. Figure 3 shows an example of the dispersion curve for  $\delta > \delta_{cr}$ . An inset shows the dependence of the largest unstable wave number  $k_*$  on  $\epsilon = (\delta - \delta_{cr})/\delta_{cr}$ . Numerical simulations are denoted by asterisks, the asymptote  $k_* = (0.36/m)\epsilon^{1/2}$  is shown by the dashed line.

For a very wide system the instability threshold  $\delta_{cr}$  does not depend on  $m$ . To see this, introduce new dimensionless variables  $r = (m/\delta^{1/2})R$ ,  $t = m^2 T$ , and  $u = U/m$ . In this case,  $m$  drops out of the problem. A consequence of the elimination of  $m$  is that one can easily find the dependence of the velocity,  $v$ , and of the wave number,  $k$ , on  $m$ :  $v = m^{-1}\delta^{-1/2}V$ ,  $k = m^{-1}\delta^{1/2}K$ . Since the scaled front velocity,  $V$ , and the scaled wave number,  $K$ , must be independent of  $m$ ,  $v$  and  $k$  are proportional to  $m^{-1}$ . We will not eliminate the parameter  $m$  from the problem and will work with Eqs. (2). Different types of cells have different diffusion coefficients  $D_u$  and different proliferation rates  $\alpha$ . Therefore, it is convenient that the dependence of the physical quantities  $k_{phys} = k[D_c/(\beta u_0^2)]^{-1/2}$  and  $v_{phys} = v(D_c \beta u_0^2)^{1/2}$  on  $D_u$  and  $\alpha$  enters only via the dimensionless variables  $v$  and  $k$ .

For a system of finite width we need to form a discrete set of modes from the modes of the infinite-width system by imposing  $kL = 2n\pi$ , where  $n = 1, 2, \dots$  and  $L$  is the width of the system. For a small enough system we can ‘freeze out’ the instability if  $k_* < 2\pi/L$ . For a spherical tumor  $L$  is of the order of the diameter. For example, Figure 1(a), could correspond to small  $k_*$ .

We now consider a phase plane of parameters  $(\delta, m)$ , see Fig. 4. As mentioned above, the main differences between the experiments with wild-type and mutant cells are in the velocity of the front propagation and possible symmetry-breaking. It means that the region of larger  $v$  and smaller  $k_*$  in this phase plane corresponds to wild-type cells, while the region of smaller  $v$  and larger  $k_*$  corresponds to mutant cells, see Fig. 4.

We consider two families of curves: the first is of constant front velocity  $v = \text{const}$  and the second is of constant largest unstable wave numbers  $k_* = \text{const}$ . We focus first on  $v = \text{const}$  curves. It was shown previously, that for  $m = 1$  and large  $\delta$ ,  $v = 1.219\delta^{-1}$  [14]. Combining this with the  $m$  dependence, one can see that in the  $(\delta, m)$  phase plane the curves of constant velocities for large  $\delta$  are given by  $\delta = \text{const}/m$ . Then, we consider  $k_* = \text{const}$  curves. Our numerical calculations indicate that for large values of  $\delta$ , the largest unstable wave number  $k_*$  tends to some constant independent of  $\delta$ ; the value of this constant for  $m = 1$  is approximately 0.5. Therefore, for large  $\delta$ ,  $k_* = 0.5/m$ , and the curves of constant  $k_*$  are given by  $m = \text{const}$ . Figure 4 shows also these large  $\delta$  asymptotes. A typical length scale is  $[D_c/(\beta u_0^2)]^{1/2} \sim 0.2 \text{ cm}$  and a typical velocity scale  $(D_c \beta u_0^2)^{1/2} \sim 4 \times 10^{-7} \text{ cm/s}$ .

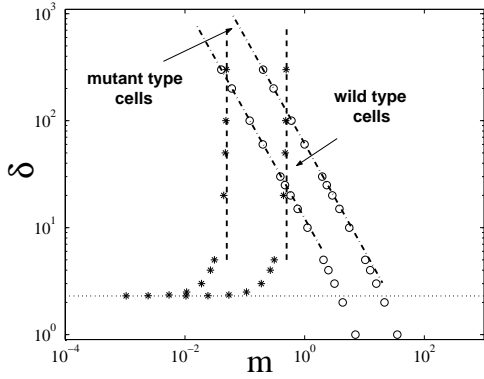


FIG. 4: The phase plane  $(\delta, m)$  with two families of curves:  $v = \text{const}$  and  $k_* = \text{const}$ , calculated from Eqs. (3) and (5). The two curves marked by  $\circ$ 's show  $v = \text{const}$ ;  $v = 0.1$  (left), and  $v = 0.02$  (right). The two curves marked by  $*$ 's show  $k_* = \text{const}$ . The left-hand curve corresponds to a stronger instability,  $k_* = 10$ , while the right one corresponds to a weaker instability,  $k_* = 1$ . Also shown are the large  $\delta$  asymptotes:  $\delta = \text{const}/m$  for  $v = \text{const}$  curves, and  $m = \text{const}$  for  $k_* = \text{const}$  curves, see text. The instability threshold for an infinite stripe,  $\delta \approx 2.300$ , is plotted by the dotted line. The larger- $\delta$  and smaller- $m$  region correspond to wild-type cells, while mutant cells are in the region of smaller  $\delta$  and larger  $m$ . This suggests that wild-type cells have a larger diffusion constant, but a smaller proliferation rate, compared to mutant cells.

Comparing this with experimental data [6], one can see that the dimensionless wave number  $k_*$  and front velocity  $v$  should be of the order of 5 and 0.1, correspondingly.

As one can see on Fig. 4, larger- $\delta$  and smaller- $m$  region corresponds to wild-type cells, while mutant type cells correspond to smaller- $\delta$  and larger- $m$  region. Thus we predict that wild-type cells have a larger diffusion constant but a smaller proliferation rate than mutant cells in the invasive zone. Comparing these theoretical predictions with experiments [6], two points should be taken into account. First, experiments [6] with tumor cells were performed in a three-dimensional geometry, so the tumor growth can be described by spherical propagating fronts for wild-type cells. In order to explain branching patterns of mutant type cells, linear stability analysis of spherical fronts, rather than plane fronts, should be performed. In this case, the role of the initial tumor radius should be analyzed. Second, the basic solutions of our model are plane fronts which propagate with constant velocity. However, in experiments, the more dense inner proliferative region grows slower than the less dense outer invasive region [6]. Probably the tumors are in a transient regime, and the steady-state behavior will set in later [15]. However, our qualitative predictions should hold in three dimensions. Experimental verification of these features of the growth should be possible.

In summary, we have considered the growth of GBM tumors. *In vitro* experiments [6] showed that the dynam-

ics of growth and resulting patterns are quite different for wild-type and mutant cells. For the wild-type the invasive region grows faster, and tumor remains spherically symmetric. On the other hand, the invasive region grows slower for the mutant cells, and there are indications of symmetry-breaking of spherically symmetric growth. We formulated a simple reaction diffusion model that captures these experimental findings. Based on our model, we explain different patterns by different diffusion constants and proliferation rates of wild-type and mutant cells: wild-type cells diffuse faster, but have a lower proliferation rate in the invasive zone. We think that an attempt should be made to test these predictions and relate them to the microscopic biology of the two cell lines.

We would like to thank Andy Stein for many useful conversations and T. Demuth and M. Berens for experimental results. Supported by NIH Bioengineering Research Partnership grant R01 CA085139-01A2.

- 
- [1] T.S. Surawicz, F. Davis, S. Freels, E.R. Laws, and H.R. Menck, *J. Neurooncol.* **40**, 151 (1998); F.G. Davis, S. Freels, J. Grutsch, S. Barlas, and S. Brem, *J. Neurosurg.* **88**, 1 (1998).
  - [2] T. Demuth and M.E. Berens, *J. Neurooncol.* **70**, 217 (2004).
  - [3] M. Huncharek and B. Kupelnick, *Oncol. Res.* **12**, 107 (2000).
  - [4] M. Nagane, H. Lin, W.K. Cavenee, H.-J. S. Huang, *Canc. Lett.* **162**, S17 (2001).
  - [5] T.S. Deisboeck, M.E. Berens, A.R. Kansal, S. Torquato, A.O. Stemmer-Rachamimov, E.A. Chiocca, *Cell Prolif.* **34**, 115 (2001).
  - [6] A. Stein, D. Mobley, T. Demuth, M.E. Berens, and L.M. Sander, unpublished.
  - [7] G.I. Sivashinsky, *Ann. Rev. Fluid Mech.* **15**, 179 (1983).
  - [8] E. Ben-Jacob and I. Cohen, *Adv. Phys.* **49**, 395 (2000); I. Golding, Y. Kozlovsky, I. Cohen, and E. Ben-Jacob, *Physica A* **260**, 510 (1998).
  - [9] L.M. Sander, T.S. Deisboeck, *Phys. Rev. E* **66**, 051901 (2002).
  - [10] A. Giese, M.A. Loo, N. Tran, D. Haskett, S.W. Coons, and M.E. Berens, *Int. J. Cancer* **67**, 275, (1996); A. Giese, R. Bjerkvig, M.E. Berens, and M. Westphal, *J. Clin. Oncol.* **21**, 1624 (2003).
  - [11] C.K.N. Li, *Cancer* **50**, 2066 (1982).
  - [12] D. Horwath, V. Petrov, S.K. Scott, and K. Showalter, *J. Chem. Phys.* **98**, 6332 (1993); A. Toth, D. Horvath, E. Jakab, J.H. Merkin, and S.K. Scott, *J. Chem. Phys.* **114** 9947 (2001); E. Jakab, D. Horvath, A. Toth, J.H. Merkin, and S.K. Scott, *Chem. Phys. Lett.* **342** 317 (2001).
  - [13] A. Malevanets, A. Careta, and R. Kapral, *Phys. Rev. E* **52** 4724 (1995).
  - [14] J. Billingham and D.J. Needham, *Philos. T. Roy. Soc.* **334**, 1 (1991).
  - [15] E. Khain, L.M. Sander, and A. Stein, unpublished.